Rock and Soil Mechanics

Volume 44 | Issue 5 Article 7

8-21-2023

Dynamic response and characteristics of tapered rigid core composite cement- soil piles under cyclic loading

Jie HE
College of Civil Engineering, Hunan University of Technology, Zhuzhou, Hunan 412007, China

Duan-wei GUO
College of Civil Engineering, Hunan University of Technology, Zhuzhou, Hunan 412007, China

De-xin SONG
Hunan No.2 Engineering Co., Ltd., Changsha, Hunan 410015, China

Meng-xin LIU
College of Civil Engineering, Hunan University of Technology, Zhuzhou, Hunan 412007, China

See next page for additional authors

Follow this and additional works at: https://rocksoilmech.researchcommons.org/journal

 Part of the Geotechnical Engineering Commons

Recommended Citation

HE, Jie; GUO, Duan-wei; SONG, De-xin; LIU, Meng-xin; ZHANG, Lei; and WEN, Qi-feng (2023) "Dynamic response and characteristics of tapered rigid core composite cement- soil piles under cyclic loading," *Rock and Soil Mechanics*: Vol. 44: Iss. 5, Article 7.
DOI: 10.16285/j.rsm.2022.5870
Available at: https://rocksoilmech.researchcommons.org/journal/vol44/iss5/7

This Article is brought to you for free and open access by Rock and Soil Mechanics. It has been accepted for inclusion in Rock and Soil Mechanics by an authorized editor of Rock and Soil Mechanics.

Dynamic response and characteristics of tapered rigid core composite cement-soil piles under cyclic loading

Authors

Jie HE, Duan-wei GUO, De-xin SONG, Meng-xin LIU, Lei ZHANG, and Qi-feng WEN

This article is available in Rock and Soil Mechanics: https://rocksoilmech.researchcommons.org/journal/vol44/iss5/7

Rock and Soil Mechanics 2023 44(5): 1353−1362 ISSN 1000−7598
https: //doi.org/10.16285/j.rsm.2022.5870 http://rocksoilmech.researchcommons.org/journal

Dynamic response and characteristics of tapered rigid core composite cement-soil piles under cyclic loading

HE Jie[1], GUO Duan-wei[1], SONG De-xin[2], LIU Meng-xin[1], ZHANG Lei[1], WEN Qi-feng[1]

1. College of Civil Engineering, Hunan University of Technology, Zhuzhou, Hunan 412007, China

2. Hunan No.2 Engineering Co., Ltd., Changsha, Hunan 410015, China

Abstract: Tapered rigid core composite cement-soil pile is an emerging type of composite pile. In order to investigate its bearing behavior in engineering applications such as highways and railways under long-term cyclic loading, model tests were conducted on four composite piles with different pile core wedge angles, static loading ratios and cyclic loading ratios. The ultimate bearing capacity under static loading as well as the cumulative settlement, pile axial force distribution, tip resistance and side friction resistance were evaluated. The results indicated that the bearing capacity of tapered inner core composite piles under static loading was better than that of constant cross-section inner core composite piles. The cumulative settlement of composite piles increased with the increase of static loading ratio and cyclic loading ratio, and can be classified into three types of stability, development and failure under different combinations of dynamic and static loading. At the same time, the value range of load satisfying each type was also given. The interaction between the core pile and the cement-soil outer pile was not noticeably diminished, and the composite pile with a tapered core pile could fully mobilize the side friction resistance of the upper soil around the pile sides and effectively reduce the stress concentration at the tip of the core pile. Therefore, its ability to resist cyclic loading was better than that of the composite pile with a constant cross-section core pile.

Keywords: tapered rigid core composite cement-soil pile; cyclic loading; ultimate bearing capacity; cumulative settlement; pile stress stress

1 Introduction

Highway and railroad engineering projects are subjected to long-term cyclic vehicle loading. Due to the low strength, high compressibility and low permeability of soft clay below the roadbed, large differential settlement may occur when the long-term cyclic load is transmitted to the soft clay foundation, leading to engineering accidents and economic losses. As an effective method of soft ground treatment, the soil-cement mixing pile refers to the construction method of the soil mixing wall (SMW). The tapered rigid core composite cement-soil pile is made by pressing a tapered core pile into a cement-soil mixing pile before the initial setting. This new composite pile not only makes full use of the advantages of tapered pile sections, but also utilizes the co-stress characteristic of the rigid core composite pile, which is of practical significance for engineering applications.

At present, scholars have studied the cumulative settlement and bearing capacity of monopiles with different types and composite foundations under cyclic loading. Chen et al.[1] analyzed the ultimate bearing capacity and cumulative settlement characteristics of pipe piles under different load combinations by conducting field tests on the prestressed concrete pipe piles. Wang et al.[2–3] used Laplace transform and impedance transfer method to obtain the pile top dynamic response and found that the tapered angle and pile length had a large effect on the dynamic response of tapered piles and a critical pile diameter ratio was existed. Wang et al.[4] carried out vertical cyclic loading tests for a monopile in calcareous sand and provided equations for pile bearing capacity and side friction resistance. Huang et al.[5] investigated the degradation of monopile axial bearing capacity under cyclic loading and verified it via numerical simulation. Lu et al.[6] carried out cyclic loading model tests on the X-section piles in the sand ground, and found that the larger the cyclic load ratio and the loading frequency were, the greater the pile top settlement was, and the dynamic stiffness at the pile top and side friction resistance was weakened. Matos et al.[7] investigated the cumulative settlement characteristics of pile models with different spacing in sand under cyclic loading and gave a numerical simulation calibration method. Gu et al.[8] and Sun et al.[9–10] carried out model tests in sand foundations and analyzed the effects of load amplitude and vibration waveform on the dynamic characteristics of XCC pile-raft composite foundations. Bekki et al.[11] studied the variation of the ultimate bearing capacity of model piles in sand under long-term cyclic loading and found that the ultimate bearing capacity of pile foundations first weakened and then strengthened under cyclic loading at a large number of cycles. Zhang et al.[12] carried out a study on the geogrid-encased stone column-improved composite foundation under cyclic loading and discussed the effects of ground treatment form, sand cushion thickness and tensile strength of geogrid sleeve on the dynamic

Received: 9 June 2022 Accepted by: 27 July 2022
This work was supported by the Natural Science Foundation of Hunan Province (2020JJ6007).
First author: HE Jie, male, born in 1976, PhD, Professor, Master tutor, mainly engaged in the research of soil mechanics and foundation. E-mail: 82017333@qq.com
Corresponding author: GUO Duan-wei, male, born in 1998, Master student, majoring in foundation engineering. E-mail: 1483259833@qq.com

characteristics of the composite foundation. Buckley et al.[13−14] investigated the variation of pile side friction resistance in chalk. They found that the reduction of the pile side effective stress led to the decrease of pile side friction resistance, and a prediction method for the pile top settlement was proposed. Zhou et al.[15] and Baghini et al.[16] predicted the pile response under cyclic loading by means of new models. The above experiments have conducted a great deal of analysis on the dynamic behaviors of monopiles with different types and composite foundations under cyclic loading, but there is limited research on the dynamic behaviors of composite piles, especially the research on the performance characteristics of tapered rigid core composite cement-soil piles under cyclic loading.

This paper investigated the dynamic characteristics of tapered rigid core composite cement-soil piles under cyclic loading through laboratory model tests. The influence of cyclic loading ratio and static loading ratio on the cumulative settlement was investigated, and the cumulative settlement control indexes which integrated the dynamic and static loading levels were proposed. The variation of pile axial force and side friction resistance before and after cyclic loading was analyzed to provide a reference for the engineering project related to tapered rigid core composite cement-soil piles under cyclic loading.

2 Model test set-up

2.1 Test site and fill

The pile foundation model test was conducted in the box with dimensions of 2.0 m×2.0 m×2.5 m. The test soil was silty clay collected from a pit in Zhuzhou, Hunan Province. The soil was air-dried and passed through the 5 mm sieve. During the process of layered filling of the model box, every 10 cm of soil was evenly sprayed with water and compacted to control the water content at 30%. The soil was filmed and stood for 7 d after filling to eliminate unbalanced stresses. The physical and mechanical parameters of the soil are shown in Table 1.

Table 1 Physical and mechanical parameters of soil

Water content w /%	Unit weight γ /(kN • m^{-3})	Plastic index I_p	Liquid limit w_L /%	Internal friction angle φ /(°)	Cohesion c /kPa	Compression modulus E_s /MPa
27.3	17.5	19.1	36.5	18.04	8.16	2.14

2.2 Pile preparation and installation process

The pile model used in the test consisted of a core pile and a cement outer pile. The pile was 80 cm in length and 11 cm in diameter. Two core pile cross-section forms, cylindrical and tapered, were designed in the test, and the corresponding core pile dimension parameters are shown in Table 2, the model diagram of the composite pile is shown in Fig.1. The 6061 type aluminum alloy was selected as the core pile material. The material satisfied the linear elastic characteristics and had high stiffness, which could well simulate the coupling effect between the rigid inner core and the flexible cement outer pile, and its material property parameters are shown in Table 3.

Table 2 Core pile dimension parameters

No.	Pile type	Core pile length L /cm	Tapered angle θ /(°)	Pile tip diameter D_0 /mm	Pile top diameter D_1 /mm
D1	Cylinder	50	0	50	50
X1, X2, X3	Taper	50	1.146	40	60

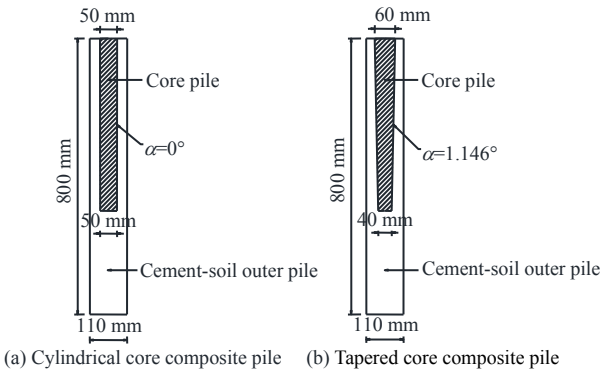

(a) Cylindrical core composite pile (b) Tapered core composite pile

Fig. 1 Composite pile model

Table 3 Physical and mechanical properties of 6061 aluminum alloy

Tensile strength R_m /MPa	Yield strength σ_s /MPa	Elongation per unit length δ /%	Elastic coefficient /GPa	Ultimate strength /MPa
⩾180	⩾110	⩾14	68.9	228

The cement-soil outer pile was obtained by mixing the cement (P.O42.5) and soil at a 15% cement mixing ratio. Referring to the actual engineering construction process, the prefabricated core pile was pressed vertically into the fully mixed cement soil and the top surface of the pile was made flush. After the composite pile was installed completely, the soil surface was covered with preservative films for 28 d before being loaded.

2.3 Loading program

The test loading was divided into static loading and cyclic loading. The static loading was achieved by a hydraulic jack, and the static loading value was controlled by a pressure sensor with a measuring range of 30 kN. The cyclic load was realized by a synchronous multi-point loading system with an actuator. Considering that the test aimed to simulate the dynamic effects of the roadbed self-weight and vehicles on the pile foundation, the loading frequency of this test was approximated as 2 Hz, and sinusoidal loading was used. The data acquisition system included the acquisitions of the pile strain, pile top cumulative settlement and pile bottom soil pressure, and the layout of the test elements is shown in Fig. 2. When the cumulative settlement at the pile top during cyclic loading exceeded 0.1D (the pile diameter $D = 11$ cm), the pile was considered to be failed[6, 17] and the loading was terminated.

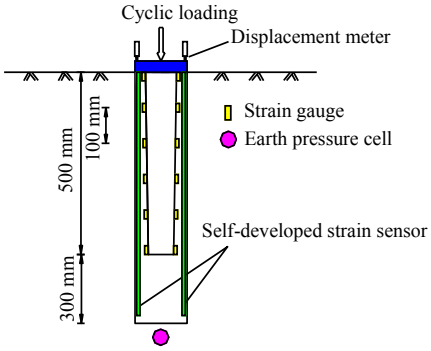

Fig. 2 Layout of test elements

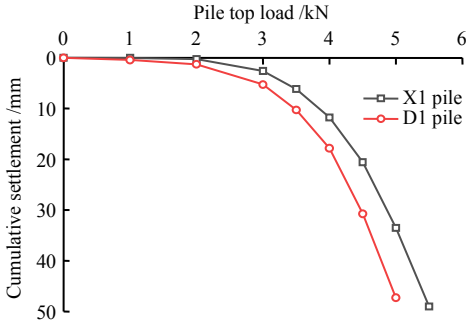

Fig. 3 Pile top load–cumulative settlement curves under static loading

Before the dynamic loading was applied, vertical bearing capacity tests were conducted for the pile models. The rapid maintenance method was used for the static loading tests, referring to the *Technical Code For Testing of Building Foundation Piles* (JGJ106—2014)[18]. A total of 16 loading cases were carried out in this test, and the cycles of each case were 5 000. The specific test loading scheme is shown in Table 4.

The static loading ratio (SLR) and the cyclic loading ratio (CLR) in this paper were defined respectively as

$$\mathrm{SLR} = P_s / P_u \tag{1}$$

$$\mathrm{CLR} = P_c / P_u \tag{2}$$

where P_s is the static load at the pile top; P_c is the cyclic load amplitude; and P_u is the ultimate bearing capacity of the composite pile.

Table 4 Loading scheme of laboratory model test

Case	Pile No.	Core pile type	Static loading value	Cyclic load ratio CLR	Actual load $Q(t)$ /kN
1-1	X1	Taper	0.1 P_u	0.1	0.0–1.0
1-2				0.2	0.0–1.5
1-3				0.3	0.0–2.0
1-4				0.4	0.0–2.5
2-1	X2	Taper	0.3 P_u	0.1	1.0–2.0
2-2				0.2	0.5–2.5
2-3				0.3	0.0–3.0
2-4				0.4	0.0–3.5
3-1	X3	Taper	0.5 P_u	0.1	2.0–3.0
3-2				0.2	1.5–3.5
3-3				0.3	1.0–4.0
3-4				0.4	0.5–4.5
4-1	D1	Cylinder	0.3 P_u	0.1	1.0–2.0
4-2				0.2	0.5–2.5
4-3				0.3	0.0–3.0
4-4				0.4	0.0–3.5

3 Results and discussion

3.1 Ultimate bearing capacity of composite piles under static load

In order to determine the static loading ratio and cyclic loading ratio and to explore the bearing characteristics of different composite pile types under static loading, vertical static loading tests were carried out on the D1 and X1 piles before cyclic loading, and the pile top load-cumulative settlement curves of the D1 and X1 piles under static loading were obtained, as shown in Fig. 3.

As can be seen from Fig.3, the pile top load–cumulative settlement curves of the test piles under static loading were of slow variation type, and the pile top cumulative settlement was small at the beginning of loading and the difference between the two piles was small. With the increase of vertical graded load, the pile top cumulative settlement gradually increased. The load corresponding to the pile top settlement of 40 mm was taken as the ultimate bearing capacity of the pile and the ultimate bearing capacity of the composite pile P_u was obtained, as shown in Table 5.

Table 5 Ultimate bearing capacity of composite pile

No.	Core pile type	Ultimate bearing capacity P_u /kN
D1	Cylinder	4.79
X1	Taper	5.21

From Table 5, the ultimate bearing capacities of the X1 pile with tapered inner core and the D1 pile with uniform cross-section inner core were 5.21 kN and 4.79 kN, respectively, and the existence of tapered angle increased the ultimate bearing capacity by 8.77%, which meant that the bearing capacity of the composite pile with tapered inner core was better than that of the composite pile with uniform cross-section inner core under static loading. Before cyclic loading, the actual values of static and dynamic loading under each case were calculated according to the measured ultimate bearing capacity of the composite pile P_u and then the load was applied. According to the data in Table 5 and in order to meet the feasibility of calculation and test operation, an approximate value of P_u=5 kN was substituted into the calculation of static and cyclic loads for each case in this paper.

3.2 Effect of cyclic load ratio and tapered angle on cumulative settlement

Figure 4 shows the variation trend of the pile top cumulative settlement with the number of cycles under different cyclic loading ratios when the static loading ratio SLR was constant (SLR equaled to 0.1, 0.3 and 0.5, respectively). At the beginning of cyclic loading, the pile top settlement was small and variation curves were approximately linear. As the number of cycles increased, the pile top settlement gradually increased and exhibited a large difference with the increase of cyclic loading ratio CLR, which indicated that the

cumulative settlement at the pile top was closely related to the cyclic loading ratio CLR. The pile side and pile tip soil in the soft clay ground under cyclic loading was in a state of constant normal stiffness[19−20], and the accumulated settlement at the pile top was the macroscopic manifestation of the above-mentioned soil elements under cyclic compression or shearing.

From Fig. 4(a), it could be seen that when the static loading ratio SLR was 0.1, the static loading level applied on the pile top was constant and small. As the cyclic loading ratio CLR increased, the total cumulative settlement at the pile top increased, and the larger the cyclic loading ratio was, the greater the increase rate of the cumulative settlement became. When the cyclic loading ratio was small (CLR =0.1), the settlement at the pile top reached 63.04% of the total settlement at the end of loading after 100 cycles, indicating that the settlement at the pile top was basically completed after a relatively small number of cycles, the settlement at the pile top increased slightly during the subsequent loading process, and the settlement at the pile top tended to be stable integrally. As the cyclic loading ratio increased (CLR =0.3 and 0.4), the settlement after 100 cycles only accounted for 15.2% and 12.0% of the total settlement respectively, indicating that the cumulative settlement continued to increase during the cyclic loading process and presented an overall development trend. It should be noted that under CLR = 0.2, the pile top settlement at the initial loading stage was less than that under CLR = 0.1. This was mainly due to the fact that the two loading conditions were applied on the same pile in succession, as a result, the soil was compressed and existed in a certain occurrence state.

As could be seen from Figs. 4(b) and 4(d), when the static loading ratio was 0.3, the static loading level at the pile top increased, and the trend of cumulative settlement with increasing cyclic loading ratio was approximately the same as that at SLR = 0.1, but the total settlement under each case was increased compared to the latter. When the cyclic load ratio was small, the cumulative settlement showed a more pronounced non-developing trend. As the cyclic loading ratio was increased, the cumulative settlement still exhibited an increasing trend. Figs. 4(b) and 4(d) showed a comparable overall trend in the cumulative settlement, although the tapered angle conditions were different. However, from Fig. 4(c), it could be found that when the static loading level continued to become larger (SLR = 0.5), the cumulative settlement hardly increased in the middle and late stages of loading under small cyclic loading. With the increase of cyclic loading ratio, the cumulative settlement increased rapidly until the failure criterion was reached, especially when the peak load was close to the ultimate bearing capacity (SLR = 0.5 and CLR = 0.4), the pile top settlement already exceeded 0.1*D* after 400 cycles.

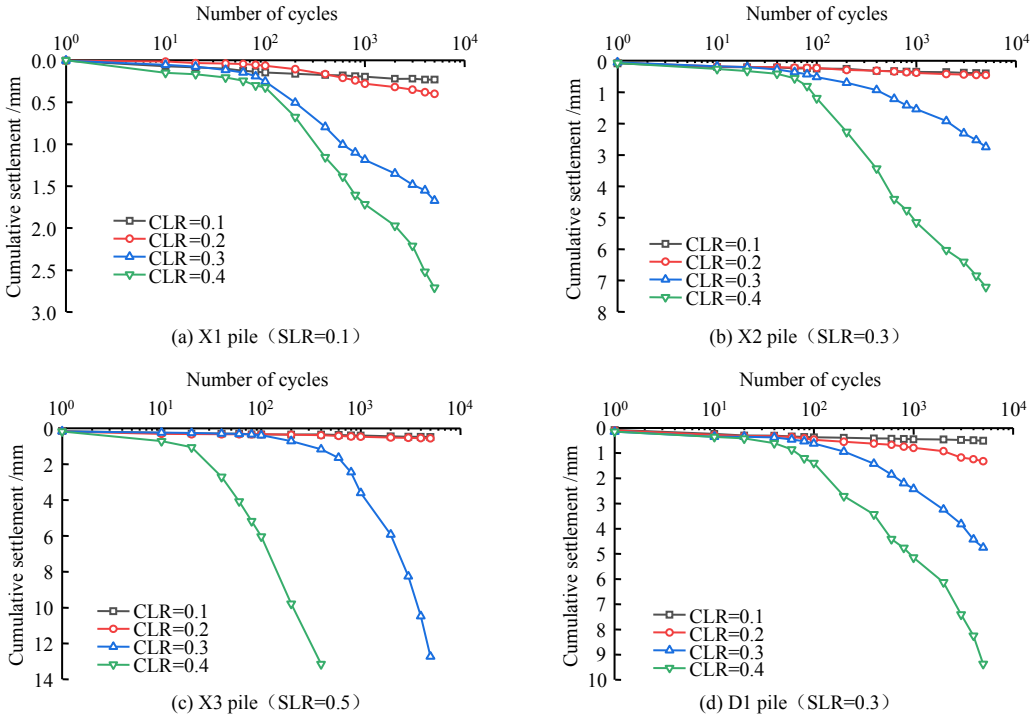

Fig. 4 Effect of cyclic loading ratio CLR on cumulative settlement

In order to analyze the effect of tapered angle on the cumulative settlement, the cumulative settlement of the composite pile with tapered core pile and the composite pile with uniform cross-section core pile are summarized in Fig. 5. It could be found in Fig. 5 that the cumulative settlement of the D1 composite pile with uniform cross-section core pile was greater than that of the X2 composite pile with tapered core pile and the increase rate of the cumulative settlement of the D1 pile was also greater than that of the X2 pile under the same load combination. CLR = 0.3 was presented as an example for analysis. The cumulative settlement of the D1 pile with uniform cross-section core pile was in a development trend, while the

cumulative settlement of the X2 pile with tapered core pile was more stable under the same cyclic load ratio, which indicated that the composite pile with tapered inner core had a stronger ability to resist cyclic loading than the composite pile with uniform cross-section inner core.

3.3 Effect of SLR on cumulative settlement

Figure 6 shows the cumulative settlement versus the number of cycles for different static loading ratios SLR at the same cyclic loading ratio CLR (0.1, 0.2, 0.3 and 0.4).

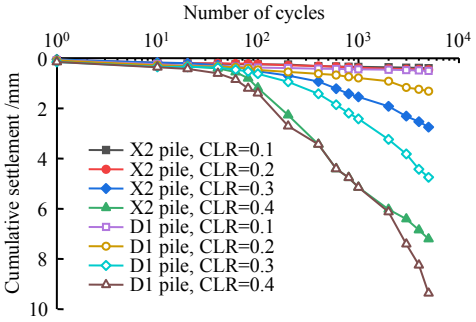

Fig. 5 Effect of tapered angle on cumulative settlement

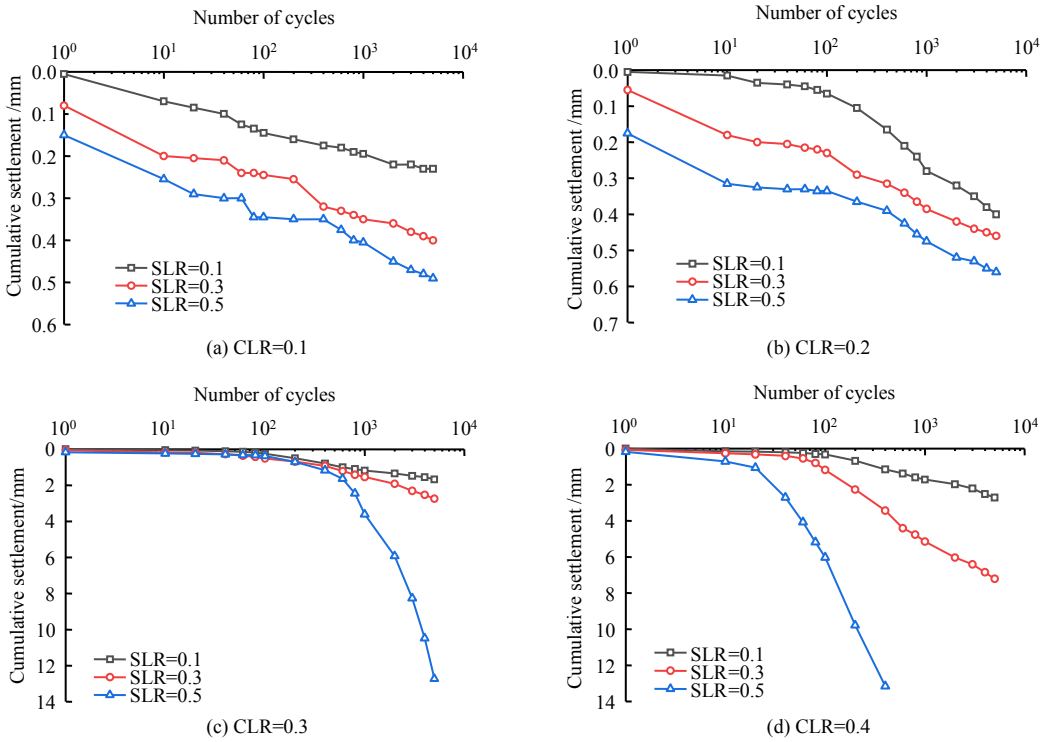

Fig. 6 Effects of static loading ratio SLR on cumulative settlement

As shown in Figs. 6(a) and 6(b), when the cyclic loading ratio CLR was small (CLR=0.1 and 0.2), the cumulative settlement was approximately linear with the number of cycles, and the total cumulative settlement was small overall and did not exceed 1 mm. With the increase of the static loading ratio SLR, the cumulative settlement rose to some extent after the same number of cycles, but the rate of increase was small and remained linear, which indicated that when the dynamic load level was small, the effect of the change of static load ratio on the cumulative settlement was not drastic. As can be seen from Figs. 6(c) and 6(d), when the cyclic loading ratio CLR was large (CLR=0.3 and 0.4), the cumulative settlement increased non-linearly. When the static loading ratio increased, the rate of increase of the cumulative settlement also changed significantly. As the static loading ratio SLR increased to 0.5, the cumulative settlement rapidly accumulated and reached the failure criterion. This indicated that the cumulative settlement was more sensitive to the static loading ratio SLR when the cyclic loading ratio CLR was large than when the cyclic load ratio SLR was small.

The comparison between Fig. 4 and Fig. 6 showed that the change of cyclic loading ratio resulted in a significant change in the development trend of cumulative settlement and the pile top settlement changed from stabilization to continuous increase or rapid failure under different static loading ratios, as shown in Fig. 4. In contrast, in Fig. 6, the effect of static loading ratio on the cumulative settlement development trend was not evident under different cyclic loading levels. When the cyclic loading was small, the cumulative settlement at the pile top always exhibited a linear development and the total settlement was small. This indicated that the cyclic loading ratio played a more important role in the pile top cumulative settlement characteristics than the static loading ratio.

3.4 Effect of number of cycles on cumulative settlement

In order to analyze the effect of the number of cycles on the cumulative settlement, the cumulative settlement was normalized to obtain the cumulative settlement ratio. The cumulative settlement ratio was defined as the ratio of the settlement after m cycles to the total cumulative settlement. Fig. 7 illustrates the

relationship curve between the cumulative settlement ratio and the number of cycles.

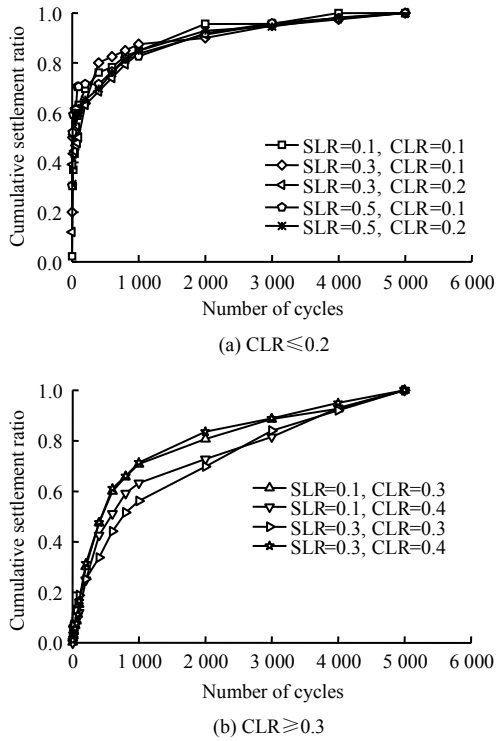

Fig. 7 Effect of number of cycles on cumulative settlement

One can see from Fig.7 that the cumulative settlement ratio increased as the number of cycles increaseed, and presented a periodic change. The cumulative settlement ratio increased rapidly at the early loading stage, but slowly at the middle and late stages of loading. In addition, the increase amplitude in the cumulative settlement ratio varied with the different dynamic loading levels.

When the cyclic load ratio CLR was small, the cumulative settlement ratio increased rapidly within a small number of cycles, and the cumulative settlement reached 70% to 80% of the total settlement after 500 cycles, while the cumulative settlement ratio increased at a smaller rate during the subsequent cyclic loading process, showing a slow accumulation or even no accumulation of the settlement at the pile top. When the cyclic loading ratio CLR was large, the increase rate of the cumulative settlement ratio within a small number of cycles was significantly smaller than that in the case of a small CLR (Fig.7(a)). The cumulative settlement ratio reached only 40%–50% of the total settlement after 500 cycles, and in the subsequent loading process, the cumulative settlement ratio increased linearly, but with a gradient smaller than that at the beginning of loading. The phenomenon indicated that under such load combinations, the pile top settlement not only increased rapidly at the beginning of loading, but also continued to accumulate at the later stages of loading.

3.5 Evaluation criteria for cumulative settlement considering only the cyclic load ratio

If only the effect of the cyclic loading ratio CLR on the cumulative settlement at the pile top was analyzed without considering the static loading effect, the existing cases could be treated approximately. Since the actual load values $Q(t)$ for some cases were the same as the actual peak load values when only the cyclic loading ratio was considered, the equivalent cyclic loading ratio without considering the effect of static loading could be obtained according to its maximum actual load value $Q(t)$, so that the critical cyclic loading ratio of the pile model could be analyzed. The equivalent cyclic loading ratio was calculated as follows:

$$n=\frac{Q(t)_{\max}}{P_{\mathrm{u}}} \tag{3}$$

where n is the equivalent cyclic loading ratio; and $Q(t)_{\max}$ is the actual maximum load. Here P_{u} was approximately taken as 5 kN, and the specific values after calculation are shown in Table 6.

Table 6 Equivalent cyclic loading ratio

Case	Pile No.	Static loading value /kN	Cyclic loading ratio CLR	Actual load $Q(t)$ /kN	Equivalent cyclic loading ratio n
1-1	X1	0.1 P_{u}	0.1	0–1.0	0.2
1-2			0.2	0–1.5	0.3
1-3			0.3	0–2.0	0.4
1-4			0.4	0–2.5	0.5
2-3	X2	0.3 P_{u}	0.3	0–3.0	0.6
2-4			0.4	0–3.5	0.7
3-3	X3	0.5 P_{u}	0.3	1.0–4.0	0.8
3-4			0.4	0.5–4.5	0.9

The cumulative settlement data under each corresponding case were collated, and the relationship between the cumulative settlement and the number of cycles under the action of equivalent cyclic loading ratio was obtained as shown in Fig. 8.

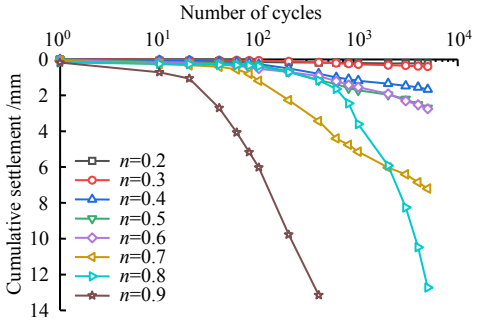

Fig. 8 Relationships between cumulative settlement and number of cycles under equivalent cyclic loading ratio

From Fig. 8, it can be seen that the cumulative settlement increased with the increase of number of cycles, the cumulative settlement was approximately linear with the number of cycles at the beginning of loading, and gradually deviated from the linear relationship in the middle and later stages of loading, and this pheno- menon became more and more obvious with the increase of the equivalent cyclic loading ratio. A large equivalent cyclic loading ratio corresponded to a great total settlement at the end of

loading and a large rate of increase of the cumulative settlement. The develop- ment trend of cumulative settlement under different equivalent cyclic loading ratios could be roughly divided into three categories: 1. when $n \leqslant 0.3$, the cumulative settlement was basically completed after a very small number of cycles, and only a small settlement was generated at the pile top in the late loading period, which could be approximated as stable; 2. when $0.3 < n \leqslant 0.7$, the cumulative settlement continued to increase during cyclic loading, but did not reach the failure criterion at the end of loading, and the cumulative settlement in this interval showed a development trend; 3. when $n > 0.7$, the cumulative settlement increased rapidly until it reached the failure criterion.

It should be noted that when $n = 0.7$, according to its trend of cumulative settlement, the cumulative settlement would reach the failure criterion if the number of cycles continued to increase. The maximum equivalent cyclic load ratio that did not cause failure was generally defined as the critical cyclic loading ratio, and a comprehensive analysis of the cumulative settlement development in this test could determine the critical cyclic loading ratio of the test pile to be between 0.6 and 0.7.

3.6 Evaluation criterion of cumulative settlement considering static load ratio and cyclic load ratio

Combining Fig. 4 and Fig. 6, it could be found that the cumulative settlement at the pile top was subject to the combined effect of static loading ratio SLR and cyclic loading ratio CLR, so it was not reasonable to merely consider the critical cyclic loading ratio as the design control criterion. In this paper, the cases of different load combinations were classified according to the development trend of cumulative settlement, and three types of cumulative settlement development were obtained, as shown in Fig. 9.

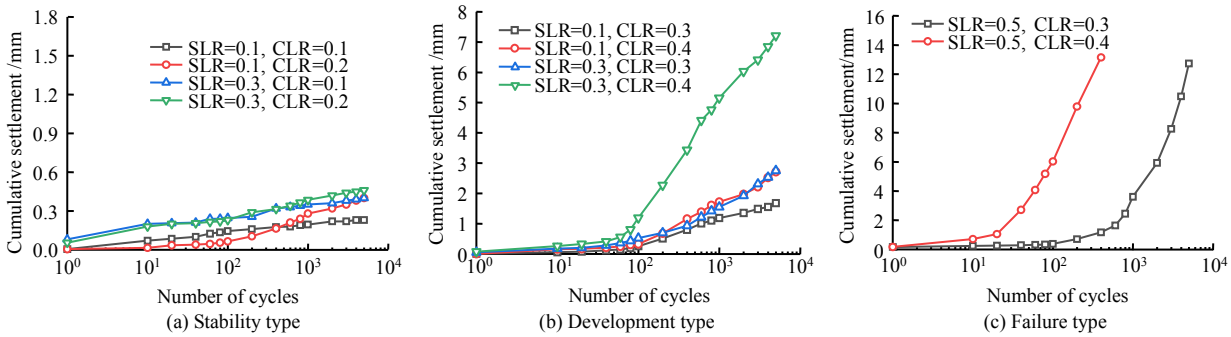

Fig. 9 Three types of cumulative settlement development

Figure 9(a) shows the cumulative settlement curves of the stability type under four different combinations of dynamic and static loading. The cyclic loading ratio of this load combination type was relatively small ($\mathrm{CLR} \leqslant 0.2$). From a macroscopic point of view, the cumulative settlement after cyclic loading with a large number of cycles was very small (not more than 1 mm) and the settlement curve was smooth and steady. This was mainly due to the fact that the cyclic compression effect on the soil at the pile tip and the cyclic shearing effect on the soil at the pile side were weak, and no obvious plastic strain was generated in the soil, at this time the pile tip resistance and side friction resistance offset the cyclic loading effect.

Figure 9(b) illustrates the cumulative settlement curves of the development type. This settlement curve type had a relatively large cyclic load compared with the stability type ($\mathrm{CLR} \geqslant 0.3$). The pile top settlement continued to accumulate during the loading process, but did not reach the failure criterion at the end of loading. The curves exhibited a nonlinear characteristic, and large SLR and CLR corresponded to a great increase rate of the cumulative settlement. For the development type curve, the plastic strain in the soil gradually accumulated under cyclic load, a tiny relative displacement was occurred at the pile-soil interface, and the pile side friction resistance appeared to weaken, thus redistributing the pile axial force.

Figure 9(c) displays the cumulative settlement curves of the failure type. The static loading ratio and cyclic loading ratio in this settlement curve type were large, and the pile top settlement continued to increase and the increase rate was fast. The failure criterion of $0.1D$ (11 mm) was reached at the end of loading or even after a smaller number of cycles. For the failure type curves, the soil at the pile side was subjected to large cyclic shearing with large relative displacement at the pile-soil interface. The side friction resistance weakened rapidly, thus the cyclic compression effect on the soil at the pile end was intensified, and the plastic strain of the soil accumulated continuously.

When considering the cumulative settlement as the pile foundation design control standard, the static load level and cyclic load level should be comprehensively considered, and the cumulative settlement distribution chart should be analyzed and divided according to the settlement development type as shown in Fig. 10. In the design of pile foundations, if the cumulative settlement of pile foundations is required to be stability type, i.e., the cumulative settlement at the pile top develops slowly after a large number of cycles, then the dynamic and static load combination should be controlled in the stability zone, and the following equation should be satisfied:

$$\left.\begin{array}{l} \mathrm{CLR} \leqslant 0.2, \quad (0 \leqslant \mathrm{SLR} \leqslant 0.3) \\ \mathrm{SLR} + 2\mathrm{CLR} \leqslant 0.7, \quad (0.3 < \mathrm{SLR} \leqslant 0.7) \end{array}\right\} \tag{4}$$

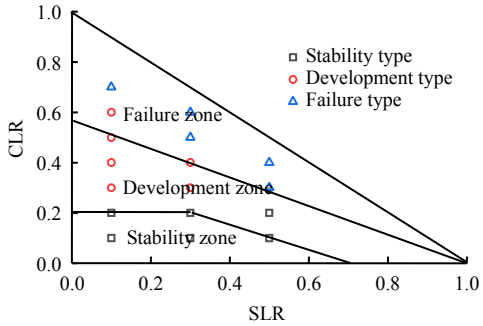

Fig. 10 Cumulative settlement distribution

If the cumulative settlement type of pile foundations is allowed to be development type, i.e., the cumulative settlement at the pile top can have a certain accumulation so that the side friction resistance and tip resistance can be fully developed, the load combination should be controlled to be located in the developmental zone and meet:

$$4\mathrm{SLR}+7\mathrm{CLR}\leqslant 1,\quad (0\leqslant \mathrm{SLR}<1) \tag{5}$$

The dynamic and static load combinations in the failure zone of the cumulative settlement distribution diagram should be avoided in the design.

3.7 Pile stress distribution under cyclic load

3.7.1 Variation of pile axial force

In order to analyze the variation of pile axial force under cyclic loading, the X1 pile was firstly taken as an example, and the load transfer mechanism of the tapered rigid core composite cement-soil pile under static load was briefly analyzed. According to the strain data of the core pile and cement outer pile collected from the test, the axial force distribution of the core pile and outer pile under static load was obtained as shown in Fig. 11, and the axial force of the core pile N_{icor} was calculated by

$$N_{\mathrm{icor}}=E_{\mathrm{cor}}A_i\varepsilon_i \tag{6}$$

where E_{cor} is the modulus of 6061 aluminum alloy core pile; A_i is the cross-section area of the core pile at the depth i; and ε_i is the strain of the cross-section at the depth i.

The axial force of the cement-soil outer pile was divided into two parts of the compound segment (N_{ic}) and the non-compound segment (N_{inc}) for calculation, and the calculation method is shown in the following equations:

$$\left.\begin{aligned}&\text{Compound segment: } N_{\mathrm{ic}}=E_i\left(A-A_i\right)\varepsilon_i\\&\text{Non-compound segment: } N_{\mathrm{inc}}=E_iA\varepsilon_i\end{aligned}\right\} \tag{7}$$

where E_i is the elastic modulus of the cement-soil at the depth i; and A is the cross-section area of the composite pile.

As shown in Fig. 11(a), the core pile axial force decreased gradually along the depth under graded static loading and decayed rapidly in the upper part of the pile. The axial force at the bottom of the core pile was close to 0 when the static loading at the pile top was small. At this time, the interface resistance of the contact surface between the core pile and the outer pile bore almost all the load. When the static loading at the pile top reached 5 kN, the core pile tip was enhanced by the supporting effect of the cement outer pile, at this time the core pile tip bearing force and interface resistance played a role together. From Fig. 11(b), it could be found that the outer pile axial force decreased along the depth in both the compound segment and non-compound segment, but there was a sudden change in the outer pile axial force at the bottom section of the core pile. This was mainly because the load shared by the core pile in the compound segment was mainly transferred to the cement outer pile in the form of interfacial resistance and core pile tip resistance, and there was a stress concentration at the bottom section of the core pile.

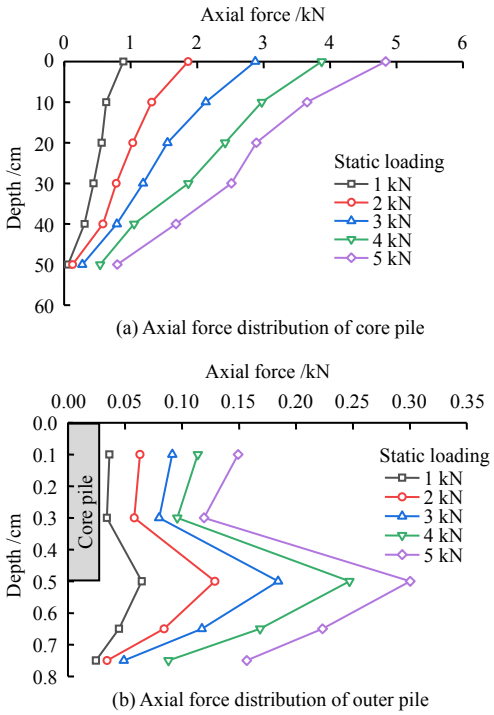

Fig. 11 Axial force distribution of X1 pile under static loading

Table 7 shows the variation in the tip axial force before and after cyclic loading for the D1 pile and X2 pile. The change of interface resistance between the core pile and cement-soil outer pile could be analyzed by the tip axial force. The table indicated that: 1. the tip axial force of the tapered core pile and uniform cross-section core pile increased slightly with the increase of peak load in both the early and late loading periods; 2. the tip axial force of the tapered core pile increased by 3.2% to 5.3%, and tip axial force of the uniform cross-section core pile increased by 1.2% to 5.2% after 5 000 cycles, i.e., the variation in the tip axial force of the core pile before and after cyclic loading was small, indicating that the bonding effect between the core pile and the cement-soil outer pile did not weaken significantly under cyclic loading; 3. the tip axial force of the tapered core pile was less than that of the uniform cross-section core pile under the same load combination, indicating that the interface resistance of the tapered core pile was better than that of the uniform cross-section core pile, i.e., the tapered core pile could effectively reduce the stress concentration at the tip of the conventional uniform cross-section core pile.

3.7.2 Variation of tip resistance

The relationship between the composite pile tip

resistance and the number of cycles under each load combination was calculated from the earth pressure cell display as shown in Fig. 12.

It was observed in Fig.12 that tip resistance increased in different degrees before and after cyclic loading, and a large cyclic load ratio corresponded to a great increase as well as a large increase rate in the tip resistance. The static loading ratio SLR=0.1 in Fig. 12(a) was presented as example for analysis. When the cyclic loading ratio was small ($CLR = 0.1$), there was a small increase in the tip resistance of the composite pile during cyclic loading, the ratio of the tip resistance to the peak load increased by 3.6%. When the cyclic loading ratio increased ($SLR = 0.1$ and $CLR = 0.4$), the ratio of the tip resistance to the load peak value increased by 11.61%, i.e., with the increase of cyclic loading, the tip resistance of the composite pile was fully mobilized after cyclic loading, meanwhile, as the static loading ratio increased, Figs.12(b) and 12(c) exhibited a similar variation trend.

3.7.3 Variation of side friction resistance

The variation of the side friction resistance before and after cyclic loading could be analyzed according to the change in the tip resistance of the composite pile. The side friction resistance ratio was defined as the ratio of the side friction resistance to the peak cyclic load at the pile top. Fig.13 shows the relationship between the side friction resistance ratio of the composite pile and the number of cycles for the three settlement types.

Table 7 Variation of axial force at the bottom of core pile before and after cyclic loading

Pile No.	Load combination	Tip axial force of core pile at 10 cycles /kN	Tip axial force of core pile at 5 000 cycles /kN	Percentage increase in axial force /%
X2	SLR=0.3, CLR=0.1	0.125	0.129	3.2
	SLR=0.3, CLR=0.2	0.214	0.225	5.1
	SLR=0.3, CLR=0.3	0.270	0.282	4.4
	SLR=0.3, CLR=0.4	0.357	0.376	5.3
D1	SLR=0.3, CLR=0.1	0.248	0.251	1.2
	SLR=0.3, CLR=0.2	0.362	0.382	3.3
	SLR=0.3, CLR=0.3	0.427	0.449	5.2
	SLR=0.3, CLR=0.4	0.734	0.762	3.8

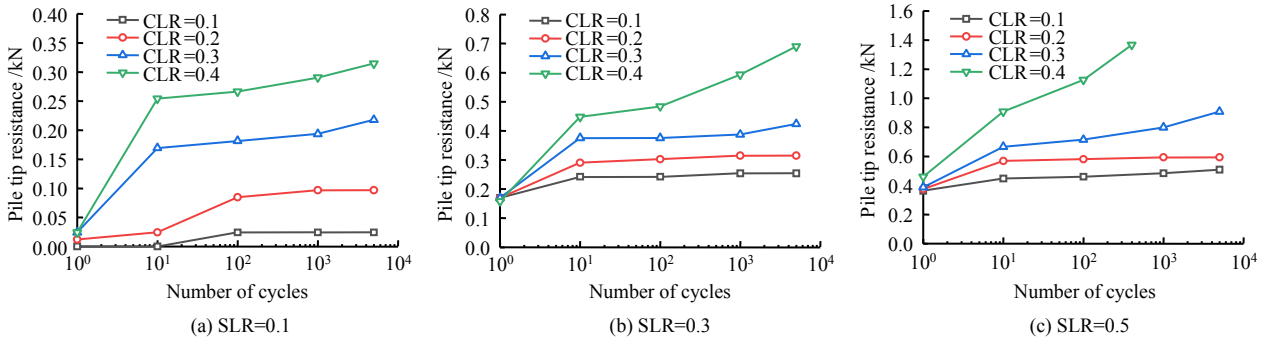

Fig. 12 Relationship between tip resistance of composite pile and number of cycles

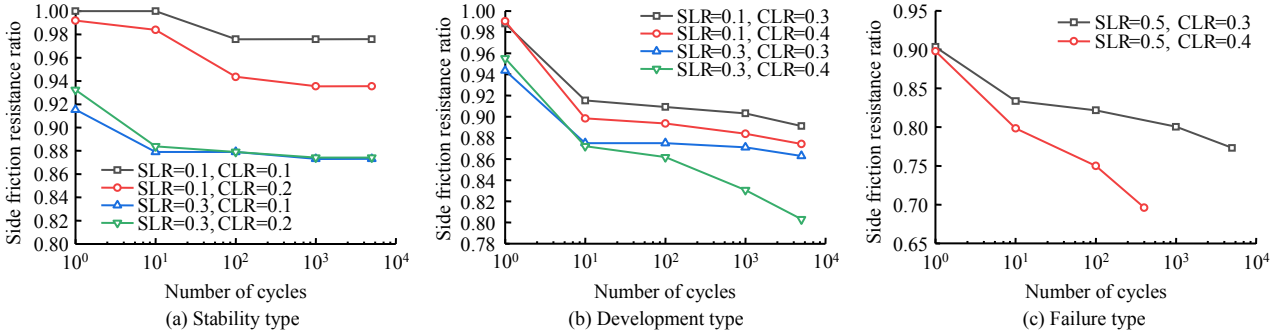

Fig. 13 Relationships between side friction resistance ratio of composite pile and number of cycles for three settlement types

As could be seen from Fig. 13, the side friction resistance ratio of the stability-type settlement decreased at the beginning of loading. The side friction resistance ratio reduced by 2.4% to 5.8% after 5 000 cycles. However, after 100 cycles, the side friction resistance ratio barely changed with the number of cycles. The finding indicated that the plastic strain accumulation of the soil adjacent to the pile side was completed within a small number of cycles for the stability-type settlement, the side friction resistance was sufficient to resist the cyclic loading and did not significantly decay in the later cyclic loading process. In contrast, for the development-type settlement, the side friction resistance ratio continued to decrease during the loading process. The side friction resistance ratio decreased by 8.47% to 15.22% after 5 000 cycles. The soil near the pile side was subject to the cyclic shearing effect, the soil particles were rearranged and the plastic strain gradually increased. The pile side friction resistance was weakened and insufficient to resist cyclic loading, which caused the pile tip to bear more load and was macroscopically manifested by a continuous increase in the cumulative settlement at the pile top. The decrease rate of the side friction resistance

ratio for the failure-type settlement was large, and the side friction resistance ratio reduced by 13.01% to 20.16% after 5 000 cycles. At this time, the plastic strain in the soil around the pile side was rapidly accumulated, resulting in a rapid decay in the pile side friction resistance. The pile tip bore more than 20% of the load, which at a macro level showed a rapid increase in the pile top settlement until the failure criterion was reached.

4 Conclusion

Through the model test of four composite piles, the cumulative settlement and pile stress of tapered rigid composite core cement-soil piles under various load combinations were monitored, and the following conclusions were obtained:

(1) The cumulative settlement of tapered rigid core composite cement-soil piles was closely related to the cyclic loading ratio CLR. When the static loading level was fixed, the larger the cyclic loading ratio was, the greater the total cumulative settlement at the pile top and the faster the increase rate of the cumulative settlement became. The cumulative settlement showed a stable trend when the CLR was small and a development trend when the CLR was large. The ability of the composite pile with tapered core to resist cyclic loading was stronger than that of the composite pile with uniform cross-section core.

(2) The cumulative settlement was also related to the static loading ratio SLR, and the cumulative settlement increased with the increase of static load ratio SLR. When the dynamic loading level was small, the change in SLR had a small impact on the increase rate of the cumulative settlement and the increase rate of the cumulative settlement changed significantly with the variation of SLR when the dynamic loading level was large.

(3) Based on the development trend of the cumulative settlement under different load combinations, the cumulative settlement could be divided into stability type, development type and failure type, and the cumulative settlement distribution was drawn according to the three types. In the design, the stability type should meet $CLR \leqslant 0.2(0 \leqslant SLR \leqslant 0.3)$ or $SLR + 2CLR \leqslant 0.7(0.3 < SLR \leqslant 0.7)$, the development type should satisfy $4SLR + 7CLR \leqslant 1.0(0 \leqslant SLR < 1.0)$ and the load combinations located in the failure zone should be avoided.

(4) The adhesion between the core pile and the cement outer pile under cyclic loading did not significantly weakened, the tapered core pile could effectively reduced the stress concentration that occurred at the tip of the traditional core piles with uniform cross-section, and the interface resistance of the tapered core pile was better than that of the core pile with uniform cross section. With the increase of cyclic load ratio, the tip resistance of the composite pile was increased to some extent, the pile side friction resistance appeared to be weakened, and the weakening degree of the failure settlement type was greater than that of the stability and development settlement types.

References

[1] CHEN Ren-peng, PENG Chun-yin, WANG Jian-fu, et al. Accumulated settlement characteristics of pipe piles in soft clay under axial cyclic loading[J]. China Civil Engineering Journal, 2021, 54(3): 119–128.

[2] WANG Kui-hua, TONG Wei-feng, XIAO Luo, et al. Study on dynamic response of tapered pile and model test[J]. Journal of Hunan University (Natural Sciences), 2019, 46(5): 94–102.

[3] WANG Kui-hua, TONG Wei-feng. Dynamic response of tapered pile based on non-equal-section pile model[J]. Journal of Harbin Institute of Technology, 2019, 51(8): 104–110.

[4] WANG S, LEI X, MENG Q, et al. Model tests of single pile vertical cyclic loading in calcareous sand[J]. Marine Georesources & Geotechnology, 2021, 39(6): 670–681.

[5] HUANG M, LIU Y. Axial capacity degradation of single piles in soft clay under cyclic loading[J]. Soils and Foundations, 2015, 55(2): 315–328.

[6] LU Yi-wei, DING Xuan-ming, LIU Han-long, et al. Model test of vertical bearing characteristics of X-section pile under cyclic loading[J]. Rock and Soil Mechanics, 2016, 37(Suppl.1): 281–288.

[7] MATOS R, PINTO P, REBELO C, et al. Axial monotonic and cyclic testing of micropiles in loose sand[M]. [S. l.]: ASTM International, 2018.

[8] GU Hong-wei, KONG Gang-qiang, LIU Han-long, et al. Dynamic response of single pile-raft composite foundation influenced by different waveforms[J]. Rock and Soil Mechanics, 2015, 36(Suppl.2): 303–309.

[9] SUN Guang-chao, LIU Han-long, KONG Gang-qiang, et al. Model tests on effect of vibration waves on dynamic response of XCC pile-raft composite foundation[J]. Chinese Journal of Geotechnical Engineering, 2016, 38(6): 1021–1029.

[10] SUN Guang-chao, KONG Gang-qiang, LIU Han-long, et al. Experimental study on load amplitude impact on dynamic response of XCC pile−raft composite foundation[J]. Journal of Central South University (Science and Technology), 2020, 51(2): 499–506.

[11] BEKKI H, CANOU J, TALI B, et al. Evolution of local friction along a model pile shaft in a calibration chamber for a large number of loading cycles[J]. Comptes Rendus Mécanique, 2013, 341(6): 499–507.

[12] ZHANG Ling, XU Ze-yu, ZHAO Ming-hua. Experimental research on behaviors of geogrid-encased stone column-improved composite foundation under cyclic loads[J]. Chinese Journal of Geotechnical Engineering, 2020, 42(12): 2198–2205.

[13] BUCKLEY R M, JARDINE R J, KONTOE S, et al. Ageing and cyclic behaviour of axially loaded piles driven in chalk[J]. Géotechnique, 2018, 68(2): 146–161.

[14] BUCKLEY R M, JARDINE R J, KONTOE S, et al. Effective stress regime around a jacked steel pile during installation ageing and load testing in chalk[J]. Canadian Geotechnical Journal, 2018, 55(11): 1577–1591.

[15] ZHOU W, WANG L, GUO Z, et al. A novel tz model to predict the pile responses under axial cyclic loadings[J]. Computers and Geotechnics, 2019, 112: 120–134.

[16] BAGHINI E G, TOUFIGH M M, TOUFIGH V. Application of DSC model for natural-element analysis of pile foundations under cyclic loading[J]. International Journal of Geomechanics, 2019, 19(7): 04019066.

[17] JARDINE R J, STANDING J R. Field axial cyclic loading experiments on piles driven in sand[J]. Soils and Foundations, 2012, 52(4): 723–736.

[18] China Academy Building Science. JGJ 106 − 2014 Technical code for testing of building foundation piles[S]. Beijing: China Building Industry Press, 2014.

[19] SIM W W, AGHAKOUCHAK A, JARDINE R J. Cyclic triaxial tests to aid offshore pile analysis and design[J]. Proceedings of the Institution of Civil Engineers-Geotechnical Engineering, 2013, 166(2): 111–121.

[20] MORTARA G, MANGIOLA A, GHIONNA V N. Cyclic shear stress degradation and post-cyclic behaviour from sand–steel interface direct shear tests[J]. Canadian Geotechnical Journal, 2007, 44(7): 739–752.